

Towards Unsupervised Speech Recognition Without Pronunciation Models

Junrui Ni, Liming Wang, Yang Zhang, Kaizhi Qian, Heting Gao, Mark Hasegawa-Johnson, *Fellow, IEEE*, Chang D. Yoo, *Senior Member, IEEE*,

Abstract—Recent advancements in supervised automatic speech recognition (ASR) have achieved remarkable performance, largely due to the growing availability of large transcribed speech corpora. However, most languages lack sufficient paired speech and text data to effectively train these systems. In this article, we tackle the challenge of developing ASR systems without paired speech and text corpora by proposing the removal of reliance on a phoneme lexicon. We explore a new research direction: word-level unsupervised ASR. Using a curated speech corpus containing only high-frequency English words, our system achieves a word error rate of nearly 20% without parallel transcripts or oracle word boundaries. Furthermore, we experimentally demonstrate that an unsupervised speech recognizer can emerge from joint speech-to-speech and text-to-text masked token-infilling. This innovative model surpasses the performance of previous unsupervised ASR models trained with direct distribution matching.¹

Index Terms—Unsupervised speech recognition; unsupervised speech segmentation.

I. INTRODUCTION

Recent advancements in speech pre-training methods and models have significantly improved supervised speech recognition, achieving impressive phone and word error rates for several high-resource languages [1]–[3]. However, these systems rely on abundant transcribed speech, making them impractical for low-resource languages. In extreme cases, there may be no parallel speech and text data available for a language. To address this, many studies have focused on using non-parallel speech and text corpora within the same language, tackling the challenge known as the unsupervised speech recognition (unsupervised ASR) problem [4]–[10].

The unsupervised ASR problem optimizes the following objective:

$$\min_{\theta} D_f[\mathbf{P}'(Y) \parallel \mathbb{E}_X[\mathbf{Q}_{\theta}(Y|X)]] \quad (1)$$

under the assumption that

$$D_g[\mathbf{P}(Y) \parallel \mathbf{P}'(Y)] < \epsilon \quad (2)$$

in an appropriate sense, where $\mathbf{Q}_{\theta}(Y|X)$ is the output distribution given input speech X over generated text Y by the recognition model with parameters θ , $\mathbf{P}(Y|X)$ is the ground-truth distribution over transcript Y given speech X , $\mathbf{P}'(Y)$ is the distribution over the unpaired text used for unsupervised learning, $\mathbf{P}(Y)$ is the distribution over ground-truth speech transcripts, and D_f and D_g are some reasonable divergence criteria to measure the distribution

mismatch. Since the speech and text are unpaired, it is challenging to recover $\mathbf{P}(Y|X)$, and we are unable to minimize Eq. (2). Note that Eq. (2) ensures that the domain difference between the speech transcript hidden from us and the text data used for unsupervised learning is small. The above formulation shows three design considerations:

- What is a reasonable granularity for the text space Y ;
- What is a reasonable representation for speech X so that we could cast X into the predicted text space Y more efficiently;
- What model and optimization algorithm serve as good candidates for minimizing $D_f[\mathbf{P}'(Y) \parallel \mathbb{E}_X[\mathbf{Q}_{\theta}(Y|X)]]$.

For the representation/granularity of the raw and predicted text space, most previous unsupervised ASR systems [4]–[8], [10] chose to work with phone-level speech features and phone-level text. While phone-level unsupervised ASR does not require paired speech and text to train, converting raw text to the phone sequences requires a grapheme-to-phone converter (G2P), and comes with the extra cost of developing a G2P converter or collecting a lexicon. While there are methods to build low-resource G2Ps with minimal resources [11], errors in the G2P system could propagate to the phone-level unsupervised ASR. Further, an unsupervised ASR system designed for the phone-level unsupervised ASR task cannot easily adapt to a lexicon-free setting, even for letter-based languages with letter-based unsupervised training [8], [12]. To reduce the reliance of unsupervised ASR systems on G2P converters, we propose solving a new task: word-level unsupervised ASR. We propose training an unsupervised ASR system that directly matches the distribution between predicted text from word-level speech features and word-level text. To constrain the problem as an early exploration, we curate a synthetic corpus that contains the top 1024 high-frequency words from the base corpus.

As we choose the text space to be word-level sequences, we need to extract word-level information from speech to efficiently minimize $D_f[\mathbf{P}'(Y) \parallel \mathbb{E}_X[\mathbf{Q}_{\theta}(Y|X)]]$. Studies have revealed that the speech representations extracted from speech foundation models pre-trained on speech-only data correlate well with underlying linguistic structures, such as phones and words [13]. Previous work shows that phone-level unsupervised ASR benefits greatly from the phone-level features extracted with these foundation models [7], [14]. In our work for word-level unsupervised ASR, we pool discretized word-level features from the speech representations extracted from two pre-trained models, HuBERT [2] and VG-HuBERT [15], in separate experiments.

Now that we have chosen the granularity of the text space and the representations of input speech, we design the model and optimization algorithm for minimizing $D_f[\mathbf{P}'(Y) \parallel \mathbb{E}_X[\mathbf{Q}_{\theta}(Y|X)]]$.

This work has been submitted to the IEEE for possible publication. Copyright may be transferred without notice, after which this version may no longer be accessible.

¹Relevant code for pre-processing, training, and evaluation will be released if the paper is accepted.

We establish a strong baseline by modifying a prior model based on the *position-unigram and skip-gram matching (PUSM)* loss [9] and propose a novel model for word-level unsupervised ASR based on *joint speech-text token-infilling (JSTTI)* with the Transformer architecture. Inspired by the recent theme in unsupervised phone-level ASR and unsupervised speech segmentation that learns the segmental structure of speech in an end-to-end fashion [10], [16], [17], we add a *differentiable boundary soft-pooler* to the JSTTI Transformer model and leverage an *external boundary refinement routine* [18] to improve the segmental structure of discretized word-level speech features. Finally, we leverage *pseudo-text self-training* to boost the performance. Every step of our pipeline reduces the word error rate, and the resulting JSTTI system significantly outperforms the baseline.

The contribution of the paper can be summarized as follows: 1) we propose word-level unsupervised ASR with unsupervised word boundaries; 2) We propose the JSTTI criterion for training word-level unsupervised ASR, and demonstrate that this criterion outperforms strong baselines; 3) we develop a full pipeline that iteratively refines the word-level segmental structure, including an end-to-end differentiable boundary detector/soft-pooler built into the JSTTI task and an external boundary self-training routine leveraging speech foundation models; 4) we modify the gradient update strategy for the PUSM model that we use as a strong baseline for the word-level unsupervised ASR task; 5) we perform extensive analysis and ablation studies for word-level unsupervised ASR, including, but not limited to, the effect of pseudo-text self-training, choice of discretized word-level speech features, and choice of model architecture for the JSTTI task. 6) we curate a simplified corpus as a first step towards word-level unsupervised ASR.

II. RELATED WORK

We discuss the recent studies on unsupervised ASR, self-supervised learning, and unsupervised speech segmentation.

Unsupervised Speech Recognition All previous studies of unsupervised ASR work with phoneme-level segmentation and phoneme-level text. Earlier models work with traditional speech features and solve the distribution matching problem in Eq. (1) with empirical output distribution matching [5] or GAN training [4], [6]. Recently, wav2vec-U [7] leverages acoustic features from speech foundation models [1], [19] and achieves competitive unsupervised ASR performance with GAN training and self-training. Later modifications remove the reliance on feature extraction heuristics [8], extend the choice of foundation models and decoding methods [14], and incorporate an iterative method that refines the phoneme boundary segmental structure with reinforcement learning [17]. Among prior work, boundary refinement has been found useful to improve the results of the unsupervised systems [5], [6], [17], which we also adopt into our system pipeline for word-level unsupervised ASR.

Our work is heavily influenced by a recent approach that applies PUSM to word-level unsupervised ASR with oracle boundaries [9]. We choose the PUSM algorithm as a strong baseline and extend the word-level unsupervised ASR task to unsupervised word boundaries. Our end-to-end boundary refinement routine driven by speech and text data is influenced by the segmental PUSM model [10], but we revised the routine to work with our JSTTI models.

Speech Representation Learning Speech foundation models pre-trained on untranscribed speech audio [1], [2], [20] have been found to provide expressive speech representation for phone-level unsupervised ASR [7], [14]. Our work on word-level unsupervised ASR utilizes the features from a pre-trained HuBERT-Large model [2], owing to a recent comparative analysis over multiple foundation models [13]. The HuBERT approach is optimized under a loss similar to the Masked Language Modeling (MLM) loss over masked discrete tokens provided by an acoustic discovery model. We also leverage VG-HuBERT [15], a visually grounded, self-supervised speech model for word discovery, trained with paired speech captions and images on top of representations from the audio and image encoders. We utilize the unsupervised word boundaries inherent within the VG-HuBERT representations to obtain word-level cluster centroids for speech quantization. We also test the VG-HuBERT features against HuBERT-Large features in one of our experiments.

There have been several successful attempts on joint speech-text pre-training [21]–[25]. Our JSTTI-based unsupervised ASR model is inspired by the earlier SpeechT5 approach [21] that does not use paired data, which is a self-supervised pre-training framework that performs joint speech/text representation learning under a shared encoder-decoder architecture to reconstruct masked speech representations and masked text spans. We have adopted many of its design choices into our JSTTI model for word-level unsupervised ASR, including the masking function and the cross-modal vector quantizer. Our work is among the first to show that joint masked reconstruction on discrete speech and text leads to an unsupervised ASR model, similar to earlier work in unsupervised machine translation [26], [27].

Unsupervised Word Segmentation for Speech We require unsupervised word boundaries for pooling word-level information. Many recent unsupervised word segmentation algorithms follow either a top-down multi-level approach by incorporating differentiable segmenters and performing contrastive predictive coding [16], [28], [29], or a bottom-up approach that discovers phone-like units and word units in separate steps [30]. There have also been statistical approaches based on the Dirichlet process on top of an instance lexicon [31]. Our JSTTI-based end-to-end boundary refinement routine can be considered as a combination of the differentiable segmenter in Segmental-CPC [16] and the differentiable soft-pooler in segmental PUSM [10], but has been developed to include the features of both.

In addition to the VG-HuBERT word segmentation mentioned previously, our work borrows two additional word segmenters: GradSeg [32] and XLS-R fine-tuning on unsupervised word boundaries [18]. GradSeg trains a ridge regression classifier on top of the extracted wav2vec 2.0 features to predict the binary labels from quantizing temporal feature gradients, with some post-processing to obtain boundary predictions from the classifier. The XLS-R fine-tuning method finetunes the XLS-R model on top of unsupervised word boundaries provided by top-tier word segmentation systems. It consistently improves the baseline performance of all previous systems on seen and unseen languages. In our work, we fine-tuned the XLS-R model on top of word boundaries provided by GradSeg on our curated small vocabulary word-level speech corpus, with another run of XLS-R boundary refinement on top of word boundaries from our end-to-end JSTTI boundary refinement model.

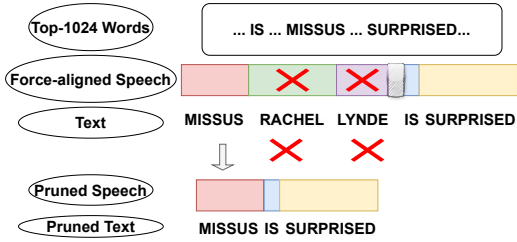


Fig. 1. We keep only the top 1024 words in the clean subset of LibriSpeech using forced alignments and respectively pre-process the transcripts.

III. METHOD

A. Curating the Corpus

We conduct experiments on the clean subset of the LibriSpeech corpus [33]. Due to the extended tail distribution of English words in the LibriSpeech corpus, we simplify the problem by *pruning the corpus so that only the top 1024 high-frequency words exist* in both the unpaired speech and text. Our curation process is shown in Figure 1, where we concatenate force-aligned speech segments corresponding to high-frequency words. On the clean subset of LibriSpeech, this pruning process removes roughly 25% of the lower-frequency word tokens.

The unpaired text corpus is constructed from the corresponding speech transcripts by removing low-frequency words. This is an idealist setting where unpaired speech and text distributions are “exact matches” of each other, given a perfect modality converter, i.e., where the divergence in Eq. (2) is zero, and $\mathbf{P}(Y) = \mathbf{P}'(Y)$. In future work, we will explore truly non-parallel settings.

B. Extracting Word-level Speech Representations

For our main results, we extract word-level speech representations from the HuBERT-Large [2] checkpoint.

As the first step, we *extract frame-level continuous features* from the 21st layer of the HuBERT-Large model, as the speech features from this specific layer are strongly correlated with word-level information [13].

Our second step involves *mean-pooling the frame-level features* within consecutive sets of word boundaries to match the average temporal granularity of corresponding word-level text. Our choice of word boundaries includes force-aligned boundaries as top-line as well as unsupervised word boundaries. We start with two unsupervised word boundary detectors: *VG-HuBERT* [15] and *GradSeg* [32]. To obtain VG-HuBERT word segmentation, we calculate the [CLS_A] token’s attention scores for all attention heads across all speech frames at the 10th layer of the VG-HuBERT₃ checkpoint. We then output attention segments as sequences of consecutive frames with attention scores in the top 30%. Finally, we predict word boundaries as midpoints between the end of one attention segment and the start of the next. To obtain GradSeg word segmentation, we first extract frame-level speech features \mathbf{f}_t out of 100 randomly selected utterances and calculate the temporal gradient magnitude as $\|\mathbf{m}_t\| = \|\frac{\mathbf{f}_{t+1} - \mathbf{f}_{t-1}}{2}\|$. We label frames with gradient magnitude in the bottom 40% as negative, as low temporal gradient magnitudes are good indicators of far-from-boundary regions [32], and the rest of the frames as positive. We then use these labels to

train a ridge regression classifier ($\text{reg}=10^7$) with inputs as mean-variance normalized \mathbf{f}_t . To obtain word boundary predictions from the scalar, continuous regression scores s_t , we follow the non-maxima suppression heuristics in [32] with a prior word frequency of 240ms per word.

For the third step, we *quantize* the continuous word-level speech feature vectors into discrete tokens using a fixed set of cluster centroids. This fixed set of cluster centroids is obtained by applying k-means clustering to the word-level features mean-pooled with unsupervised word boundaries inferred by the VG-HuBERT model, where we set $k = 1024$, the number of distinct words. Note that in our main results, we do not re-cluster the word-level feature vectors to obtain new centroids for quantization, even if the unsupervised ASR uses word boundaries from a method other than VG-HuBERT.

From now on, we will denote the discrete word-level speech cluster sequence as X and the discrete word-level text sequence as Y . The unsupervised word-level ASR models learn a distribution mapping from X to Y .

C. Establishing Baseline With PUSM

The *PUSM method* was proposed in a recent work towards word-level unsupervised speech-to-sign-language [9]. Similar to our word-level unsupervised ASR task, they clustered word-level speech features obtained from forced alignments and trained a linear generator $G(Y_t | X_t)$ defined as

$$G(Y_t | X_t) := \frac{\exp(W_{Y_t, X_t})}{\sum_{Y' \in \mathcal{Y}} \exp(W_{Y', X_t})} \quad (3)$$

for distribution matching with either word-level text or visual sign-language clusters, where Y_t denotes either a single word or sign cluster index, X_t denotes the speech cluster index and W_{Y_t} denotes the corresponding row of the matrix for G that converts the distribution of X_t to that of Y_t . During evaluation, the generator G takes each discrete speech token in the sequence as input and converts it to text or sign-language clusters by taking $\text{argmax}(\cdot)$ over the output probability vector.

The generator $G \in \mathbb{R}^{|\mathcal{X}| \times |\mathcal{Y}|}$, where its $[x, y]^{\text{th}}$ element is $G(y | x)$, is optimized using a weighted sum of two distribution matching losses. The first loss is the position-dependent unigram loss $\mathcal{L}_{\text{pos}}(G)$, defined as:

$$\mathcal{L}_{\text{pos}}(G) = \sum_{t=1}^T \left\| \hat{P}_{X_t} G - \hat{P}_{Y_t} \right\|_1 \quad (4)$$

where \hat{P}_{X_t} is the empirical unigram distribution of speech cluster indices at position t , and \hat{P}_{Y_t} is the empirical unigram distribution of textual words at position t . The second loss is the skipgram loss:

$$\mathcal{L}_{\text{skip}}(G) = \sum_{k=1}^K \left\| G^\top \hat{P}_k^{XX'} G - \hat{P}_k^{YY'} \right\|_1 \quad (5)$$

where $\hat{P}_k^{XX'}$ and $\hat{P}_k^{YY'}$ are the empirical distributions of position-independent lag- k skipgrams aggregated over speech and text token sequences, respectively. The skipgram distribution $P_k^{ZZ'}$ itself is defined as the joint distribution between two tokens that are k positions apart. To simplify our implementation, we obtain \hat{P}_{X_t} , \hat{P}_{Y_t} , $\hat{P}_k^{XX'}$ and $\hat{P}_k^{YY'}$ as unnormalized counts over the same number of speech and text sequences.

In this work, we modify the original distribution matching criterion so that it allows us to perform accurate unigram and skipgram matching on a large effective batch without running into GPU memory issues, given that the model parameters and the position unigram and skipgram parameters fit. Our *modified update strategy for PUSM* works as follows:

- 1) Define an update frequency F and a forward batch size B . The effective batch size for estimating position unigram and skipgram is then $B \times F$. Initialize the two position unigrams U_{G_x} and U_y , both of size $T \times |\mathcal{Y}|$, for saving $\hat{P}_{X_t} G$ and \hat{P}_{Y_t} , for $1 \leq t \leq T$. Initialize two skipgrams S_{G_x} and S_y , both of size $K \times |\mathcal{Y}| \times |\mathcal{Y}|$, for saving $G^\top \hat{P}_k^{X X'} G$ and $\hat{P}_k^{Y Y'}$, for $1 \leq k \leq K$ (c.f. Eqs. (4) and (5)).
- 2) For the first F update steps $1 \leq f \leq F$, keep the parameters of G fixed and aggregate the position unigrams as:

$$\begin{aligned} U_{G_x}[t,:] &= U_{G_x}[t,:] + \text{sg}\left(\hat{P}_{X_t}^{B_f} G\right) \\ U_y[t,:] &= U_y[t,:] + \hat{P}_{Y_t}^{B_f} \end{aligned} \quad (6)$$

for all positions $1 \leq t \leq T$, where $\hat{P}_{X_t}^{B_f}$ and $\hat{P}_{Y_t}^{B_f}$ are the un-normalized unigram counts for the speech and text sequences, respectively, at the position t , calculated using the f^{th} batch for speech and text, respectively. Similarly, we aggregate the skipgrams as:

$$\begin{aligned} S_{G_x}[k,:,:] &= S_{G_x}[k,:,:] + \text{sg}\left(G^\top \hat{P}_k^{X^{B_f} X^{B_f'}} G\right) \\ S_y[k,:,:] &= S_y[k,:,:] + \hat{P}_k^{Y^{B_f} Y^{B_f'}} \end{aligned} \quad (7)$$

for all skip-size $1 \leq k \leq K$, where $\hat{P}_k^{X^{B_f} X^{B_f'}}$ and $\hat{P}_k^{Y^{B_f} Y^{B_f'}}$ are the un-normalized skipgram counts for the speech and text sequences, respectively, with skip-size k . They are calculated on the f^{th} batch for speech and text, respectively.

- 3) For the second F update steps $F+1 \leq f \leq 2F$, we replay the F batches seen in the first F update steps and aggregate the gradient over the F (replayed) mini-batches after calculating the gradient of G over the following (modified) mini-batch unigram and skipgram losses for each batch:

$$\begin{aligned} \mathcal{L}_{\text{pos}}^{B_f}(G) &= \sum_{t=1}^T \left\| U_{G_x}[t,:] + \hat{P}_{X_t}^{B_f} G \right. \\ &\quad \left. - \text{sg}\left(\hat{P}_{X_t}^{B_f} G\right) - U_y[t,:] \right\|_1 \end{aligned} \quad (8)$$

$$\begin{aligned} \mathcal{L}_{\text{skip}}^{B_f}(G) &= \sum_{k=1}^K \left\| S_{G_x}[k,:,:] + G^\top \hat{P}_k^{X^{B_f} X^{B_f'}} G \right. \\ &\quad \left. - \text{sg}\left(G^\top \hat{P}_k^{X^{B_f} X^{B_f'}} G\right) - S_y[k,:,:] \right\|_1 \end{aligned} \quad (9)$$

We perform a single gradient update step to the parameters of G after collecting the gradient over all F batches.

- 4) We re-initialize U_{G_x} , U_y , S_{G_x} and S_y to all zeros and repeat steps 2 and 3.

As the stop-gradient operator $\text{sg}(\cdot)$ is used in Equation 6 and 7 in Step 2, we are no longer storing the gradient over the position unigram and skipgram losses for each sample. Instead, we only store the summed position unigram and skipgram counts. For Step 3, note that the above modification is equivalent to using a batch

size of $B \times F$ directly. For example, we can see that the skipgram loss over a large batch of $B \times F$ samples decomposes as:

$$\begin{aligned} \frac{\partial \mathcal{L}_{\text{skip}}^{B \times F}(G)}{\partial G_{xy}} &= \frac{\partial \sum_{k=1}^K \left\| \sum_{f=1}^F G^\top \hat{P}_k^{X^{B_f} X^{B_f'}} G - S_y[k,:,:] \right\|_1}{\partial G_{xy}} \\ &= \sum_{k=1}^K \text{Tr} \left(\frac{\partial \left\| \sum_{f=1}^F G^\top \hat{P}_k^{X^{B_f} X^{B_f'}} G - S_y[k,:,:] \right\|_1}{\partial \sum_{f=1}^F G^\top \hat{P}_k^{X^{B_f} X^{B_f'}} G} \right) \\ &= \sum_{k=1}^K \sum_{f=1}^F \text{Tr} \left(\frac{\partial \left\| S_{G_x-p_m}[k,:,:] - S_y[k,:,:] \right\|_1}{\partial S_{G_x-p_m}[k,:,:]} \right) \\ &= \sum_{f=1}^F \frac{\partial \mathcal{L}_{\text{skip}}^{B_f}}{\partial G_{xy}} \end{aligned} \quad (10)$$

where $\text{Tr}(X) := \sum_i X_{ii}$ is the trace of matrix X and

$$\begin{aligned} S_{G_x-p_m}[k,:,:] &:= S_{G_x}[k,:,:] + G^\top \hat{P}_k^{X^{B_f} X^{B_f'}} G - \\ &\quad \text{sg}\left(G^\top \hat{P}_k^{X^{B_f} X^{B_f'}} G\right). \end{aligned} \quad (11)$$

In our implementation, for simplicity, we set the effective batch size $B \times F$ to roughly the size of the entire speech corpus. In all our experiments, we sum the position-dependent unigram loss and the skipgram loss (both with a weight of 1), and we set $K = 4$ in Eqs. (5) and (9).

D. Proposed Model: Joint Speech-Text Token-infilling with Transformer

Inspired by SpeechT5 [21] and prior work in unsupervised NMT [26], [27], we develop a *joint speech-text token-infilling (JSTTI) approach* for word-level unsupervised ASR. The base version (i.e., without end-to-end speech-text boundary refinement introduced in Section III-E) in our main results uses a 2-layer Transformer encoder architecture (with a model dimension of 768, a position-wise feedforward dimension of 3072; and 12 attention heads) shared between the two modalities, takes masked speech or text token sequences as inputs, and predicts the masked and unmasked regions of the original sequence.

We train the JSTTI encoder model with a modified text-infilling approach of BART [34]. Specifically, we first sample spans of discrete tokens following a Poisson distribution with a mean length of 3.5, and the total length of the sampled spans is limited to less than 30% of the input sequence length. We then replace each token within 90% of the sampled spans (chosen at random) with a `<MASK>` token and each token within the remaining 10% of the sampled spans with a random token from the modality-specific vocabulary set. The specific choices of hyperparameters come from SpeechT5 [21], but because we use an encoder-only architecture, we do not change the length of the masked sequence as in BART or SpeechT5. We apply a shared Gumbel-softmax vector quantizer for a proportion of the speech and text encoder outputs across the temporal dimension [21], selected randomly with $p=0.3$. We refer

to this operation as “random mix-up.” During training, conditioned on the shared speech-text encoder representations from either speech or text, a separate speech encoder postnet calculates a weighted combination of the negative log-likelihood loss on the masked and unmasked speech tokens, and a separate text encoder postnet calculates a weighted combination of the negative log-likelihood loss on the masked and unmasked text tokens:

$$\mathcal{L}_{\text{wNLL}}^X = - \sum_{t \in \mathcal{T}_m} \log p_{E_x}(X_t | \hat{X}) - \lambda \sum_{t \in \mathcal{T}_u} \log p_{E_x}(X_t | \hat{X}) \quad (12)$$

$$\mathcal{L}_{\text{wNLL}}^Y = - \sum_{t \in \mathcal{T}_m} \log p_{E_y}(Y_t | \hat{Y}) - \lambda \sum_{t \in \mathcal{T}_u} \log p_{E_y}(Y_t | \hat{Y}) \quad (13)$$

where “wNLL” stands for “weighted NLL”, $\mathcal{T}_m/\mathcal{T}_u$ denotes the set of masked/unmasked positions, p_{E_x} denotes the speech distribution modeled by the encoder and the speech encoder postnet, and p_{E_y} denotes the text distribution modeled by the encoder and the text encoder postnet. We set $\lambda=0.5$ in all experiments. Figure 2 shows the overall architecture.

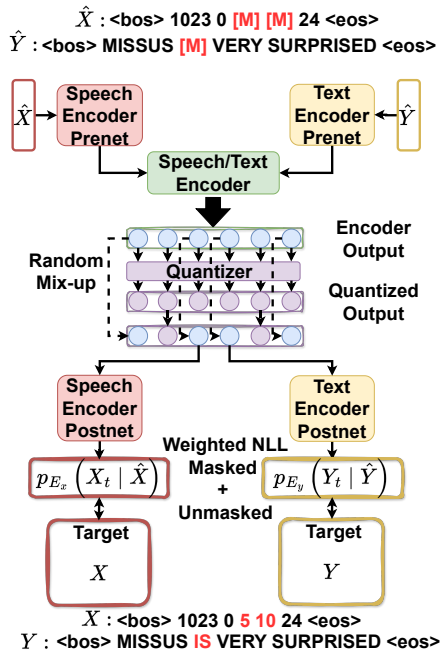


Fig. 2. The encoder-only model for speech-to-speech token infilling (left branch) and text-to-text token infilling (right branch). If N consecutive tokens are masked on the input side, they are replaced with N $\langle \text{MASK} \rangle$ tokens (denoted as [M] in the figure).

During evaluation for word-level unsupervised ASR, we found that we obtained much lower word error rates if we directly fed the speech encoder representations from the penultimate layer to the text-modality postnet instead. This choice is partially inspired by early work on unsupervised and transfer learning [35]. We believe that this evaluation choice is reasonable due to the residual nature of the Transformer layer and that the second encoder layer may have overfitted the representations of individual modalities during JSTTI training.

E. Unsupervised Word Boundary Refinement

The base JSTTI models trained with discrete word-level speech tokens extracted with VG-HuBERT or GradSeg boundaries do

not achieve good WERs. To improve the quality of word-level segmental structure for unsupervised ASR, we implement an iterative scheme that includes: 1) improving existing unsupervised word boundary predictions from GradSeg with an *XLS-R based boundary self-training method* on raw speech [18], which we denote as *wav2bnd*; and 2) adding an *end-to-end differentiable boundary soft-pooler* to the JSTTI model for *improved joint speech-text modeling*.

In the first step, we fine-tune a pre-trained 0.3B XLS-R checkpoint [3] with raw speech as input and frame-level unsupervised word boundaries provided by GradSeg as targets. We mostly follow the word boundary fine-tuning heuristics in *wav2bnd* [18]. During inference, we apply the same peak detection algorithm in *wav2bnd* on the frame-level boundary probabilities from the fine-tuned XLS-R model and tune the detection parameters so that the average number of detected words per utterance roughly aligns with the prior frequency of 240ms per word. We denote this application of *wav2bnd* on top of GradSeg boundaries as *GradSeg + wav2bnd*.

Next, we re-train the JSTTI Transformer with speech tokens extracted with *GradSeg + wav2bnd* and unpaired text. In addition, we train a small CNN network (five 1D convolution layers, with kernel size 11, 9, 7, 5, and 3 for layer one to layer five, and ReLU activation after each layer) to mimic the word boundary predictions from *GradSeg + wav2bnd* given input frame-level features. We further ask the CNN network to predict auxiliary acoustic labels jointly. These frame-level auxiliary labels are obtained by clustering the representations from the 6th layer of the HuBERT-base model. We choose the number of frame-level acoustic clusters to be 100 to match previous settings for unit-based speech resynthesis [36]. This injects additional low-level information into the CNN network and prevents overfitting to word boundary labels. Figure 3 shows how this additional CNN segmenter works during this behavior-cloning stage.

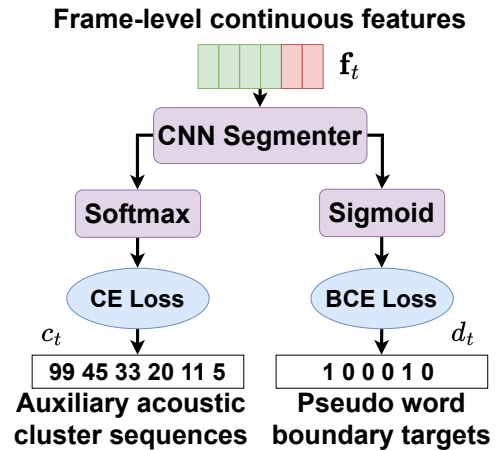


Fig. 3. We train a simple CNN classifier that takes frame-level speech features from HuBERT-Large (or VG-HUBERT in ablation studies) as input and jointly predicts the frame-level *Gradseg + wav2bnd* pseudo word boundary targets and the frame-level acoustic cluster labels as outputs. In the figure, CE stands for cross entropy loss and BCE stands for binary cross entropy loss.

After both the CNN segmenter and the JSTTI model converge, we combine them for joint fine-tuning. Figure 4 shows how the CNN segmenter converts continuous frame-level speech features into discrete speech cluster sequences in a differentiable manner. We

first describe the process we use to mean-pool within consecutive word boundaries predicted by the CNN segmenter in a differentiable manner, which we denote as the *differentiable boundary soft-pooler* [10], [16]. Let \mathbf{f}_t denote the frame-level features at frame t , and \mathbf{g}_m denote the word-level features for the m^{th} segment. We further denote $\mathbf{F} = [\mathbf{f}_1 \ \dots \ \mathbf{f}_T]^\top$, $\mathbf{G} = [\mathbf{g}_1 \ \dots \ \mathbf{g}_M]^\top$ and $\mathbf{U} \in \mathbb{R}^{M \times T}$ with all T elements in the m^{th} row being m :

$$\begin{aligned}
 \alpha_1, \dots, \alpha_T &= \text{CNN-Segmenter}(\mathbf{f}_1, \dots, \mathbf{f}_T) \\
 b_t &= \sigma(\alpha_t) + \text{sg}(\sigma(1000\alpha_t) - \sigma(\alpha_t)) \\
 s_t &= \sum_{j=1}^t b_j \\
 \mathbf{V} &= -|\mathbf{U} - [s_1 \ \dots \ s_T]| \\
 \mathbf{V}' &= 1 - \tanh(|c\mathbf{V}|) \\
 v'_m &= \sum_{t=1}^T \mathbf{V}'_{mt} \\
 \mathbf{H} &= \mathbf{V}' / [v'_1 \ \dots \ v'_m]^\top \\
 \mathbf{G} &= \mathbf{H}\mathbf{F},
 \end{aligned} \tag{14}$$

where $\sigma(x) = \frac{1}{1+\exp(-x)}$ is the sigmoid function and operations between a matrix and a vector follow their standard broadcasting rules as in Python.

We further describe the process denoted as the *differentiable k-means quantizer*, where word-level features \mathbf{g}_t go through a k-means vector quantizer with a fixed codebook $\mathbf{E} = [\mathbf{e}_1 \ \dots \ \mathbf{e}_V]$ to obtain word-level discrete speech tokens in a differentiable manner. We output a differentiable discrete index I_t for \mathbf{g}_t with the straight-through estimator trick as

$$I_t = I_{t,\text{soft}} + \text{sg}(I_{t,\text{hard}} - I_{t,\text{soft}}) \tag{15}$$

where

$$\begin{aligned}
 I_{t,\text{soft}} &= [P(\mathbf{e}_1 | \mathbf{g}_t) \ \dots \ P(\mathbf{e}_V | \mathbf{g}_t)]^\top \\
 I_{t,\text{hard}} &= \text{One-hot}(\text{argmax}_v P(\mathbf{e}_v | \mathbf{g}_t)) \\
 P(\mathbf{e}_v | \mathbf{g}_t) &= \frac{\exp(-\|\mathbf{g}_t - \mathbf{e}_v\|_2^2)}{\sum_{k \in \mathcal{V}} \exp(-\|\mathbf{g}_t - \mathbf{e}_k\|_2^2)}
 \end{aligned} \tag{16}$$

We further restrict the allowed “policy” space of the differentiable soft-pooler to mitigate instability and avoid under-segmentation and over-segmentation. The first regularization loss is the word count loss \mathcal{L}_{wc} , which restricts the total number of boundary predictions from the CNN segmenter to be close to the initial state after behavior cloning. The second loss is the word frequency loss \mathcal{L}_{wf} , which assumes that on average, every $R=12$ frames, corresponding to a duration of 240ms, would contain one boundary frame. To calculate the two losses, we use hard counts and straight-through estimators:

$$\mathcal{L}_{\text{wc}}(p_1, \dots, p_T; d_1, \dots, d_T) = \left\| \sum_{t=1}^T b_t - \sum_{t=1}^T d_t \right\|_2^2 \tag{17}$$

$$\mathcal{L}_{\text{wf}}(p_1, \dots, p_T) = \sum_{j=1}^{\lfloor \frac{T}{R} \rfloor} \left(\sum_{t=jR+1}^{(j+1)R} b_t - 1 \right)^2 \tag{18}$$

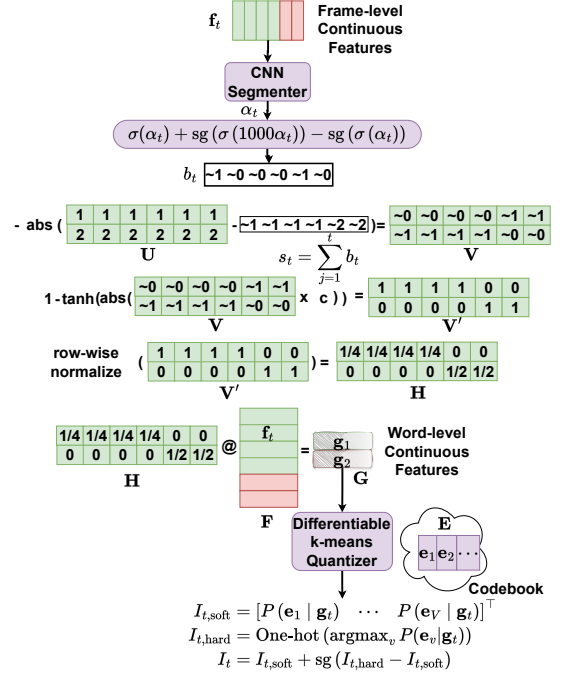


Fig. 4. An example of how the differentiable soft-pooler obtains word-level features from the boundary probability predictions of the CNN segmenter and how the speech discrete cluster sequence is obtained in a differentiable manner. The variables in the figure are referenced in the description. The symbol “ \sim ” means “a real number close to,” e.g., “ ~ 2 ” denotes a real number between 1.5 and 2.5.”

where we calculate b_t as in Eq. (14) and denote the unsupervised frame-level boundary targets used for behavior cloning as d_t .

After obtaining a differentiable version of the discrete speech tokens from the vector quantizer, we mask the tokens following the masking strategy described in Section III-D, and the unmasked version of the token sequence (with their gradients detached) serves as the target for the speech token-infilling loss (c.f. Eq. (12)). We also increase the weight of the text token-infilling loss so that the shared Transformer cannot optimize the speech loss by excessively reducing the entropy of the k-means quantizer output without making the text loss much higher. Everything else as described in Section III-D for the basic JSTTI model is left unchanged, and we denote this JSTTI-dependent word boundary refinement method on top of *GradSeg + wav2bnd* boundaries as *GradSeg + wav2bnd + JSTTI E2E-refinement*. Figure 5 shows the overall pipeline, which is trained under the a combination of $\mathcal{L}_{\text{wNLL}}^{\mathbf{X}}$, $\mathcal{L}_{\text{wNLL}}^{\mathbf{Y}}$, \mathcal{L}_{wc} and \mathcal{L}_{wf} as:

$$\mathcal{L}_{\text{JSTTI-E2E-Refinement}} = \mathcal{L}_{\text{wNLL}}^{\mathbf{X}} + \tau \mathcal{L}_{\text{wNLL}}^{\mathbf{Y}} + \gamma_1 \mathcal{L}_{\text{wc}} + \gamma_2 \mathcal{L}_{\text{wf}} \tag{19}$$

We set $\gamma_1 = 500$ and $\gamma_2 = 500000$ for our main results (c.f. Section IV-B). We increase τ from 1 to 10 for *JSTTI E2E-refinement*.

To obtain even more accurate word boundaries, we apply XLS-R word boundary self-training again, but this time using the unsupervised word boundaries extracted with our *GradSeg + wav2bnd + JSTTI E2E-refinement* method as targets for frame-level XLS-R fine-tuning. In this iteration, we also train from a larger checkpoint with 1B parameters. We extract a new set of word-level discrete speech token sequences for re-training the JSTTI Transformer encoder, and denote this setting as *GradSeg + wav2bnd + JSTTI E2E-refinement + wav2bnd-large*.

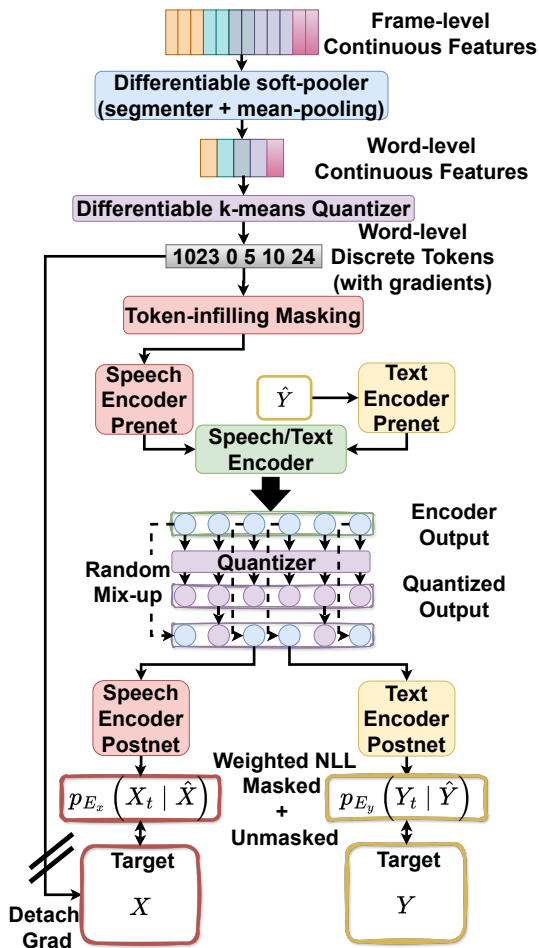


Fig. 5. Combining the differentiable soft-pooler (CNN segmenter and differentiable mean-pooling) and the differentiable k-means quantizer in Figure 4 with the original JSTTI Transformer encoder in Figure 2 gives the JSTTI E2E-refinement routine.

F. Pseudo-text Self-training

Inspired by previous work on phone-level unsupervised ASR [6]–[8], we apply *self-training on top of pseudo-transcripts*. Specifically, we fine-tune a pre-trained HuBERT-Large checkpoint under the word-level Connectionist Temporal Classification (CTC) loss, and instead of using word-level ground-truth transcripts, we use the word-level pseudo-transcripts predicted by the PUSM model or the JSTTI model. We use greedy decoding to obtain the final predicted transcripts from the fine-tuned HuBERT-Large model.

IV. EXPERIMENTS

A. Experiment Settings

All our experiments were carried out on the curated 1024-word LibriSpeech-clean subset as described in Section III-A. We kept 90% of the speech utterances (and their corresponding transcript, with the pairing relationship broken up) for unsupervised training and the rest of the utterances served as the evaluation set for reporting our results (unless denoted otherwise). The speakers in the training and evaluation set were chosen to be distinct. All PUSM models were trained under an Adam optimizer with a learning rate of 0.4, with no learning rate decay, and all JSTTI models were trained under an Adam optimizer with an initial learning rate of $2e-4$, initial

warm-up and polynomial decay. We re-initialized the optimizer for *JSTTI E2E-refinement* (c.f. Section III-E).

We used a paired validation set amounting to around 10% of the training set for recording checkpoints. For the JSTTI Transformer encoder model, we directly calculated the average validation word error rates (WER) over all validation utterances to log the best model checkpoint. The validation WERs were calculated by feeding the text output layer with speech encoder representation from the second encoder layer. This can be viewed as a surrogate supervised metric as the evaluation routine uses the speech representation from the first encoder layer instead. For the PUSM model, we directly calculated the validation WER to log the model checkpoint. We leave a detailed exploration of unsupervised validation metrics for word-level unsupervised ASR to future work.

We applied early stopping once the validation metrics converged. For PUSM models, we usually stopped before the 3000th epoch. For JSTTI models, this usually took less than 7000 epochs if we trained from scratch, and less than 1600 epochs if we initialized it from a previous checkpoint. For JSTTI E2E-refinement (c.f. Section III-E), we stopped before the 700th epoch.

For word-level speech recognition performance, we report WERs in percentage (%) for the PUSM model (denoted WER-PUSM) and the JSTTI Transformer Encoder (denoted WER-JSTTI-ENC), with word-level speech tokens extracted using different unsupervised word boundaries. We use separate flags in the table to denote WERs obtained under non-default settings. To evaluate the quality of the word boundaries, we use the standard token F1 score [37] with a tolerance of 20ms, together with precision and recall.

B. Main Results: Word-level Speech Recognition and Segmentation

TABLE I
WERs FOR PUSM AND JSTTI-ENC MODELS USING DIFFERENT WORD BOUNDARY EXTRACTORS BEFORE SELF-TRAINING. THE TOP-LINE HAS BEEN UNDERLINED AND THE BEST RESULT FOR EACH MODEL IS SHOWN IN BOLD.

Method	WER-JSTTI-ENC (↓)	WER-PUSM(↓)
<u>VG-HuBERT</u>	<u>47.99 (47.99)</u>	<u>58.73 (58.77)</u>
GradSeg	47.53 (44.76)	52.10 (50.84)
+ wav2bnd	40.45 (38.08)	44.18 (43.08)
+ JSTTI E2E-refinement	30.97 (29.39)	34.08 (33.71)
+ wav2bnd-large	28.00 (26.51)	32.11 (31.91)
GradSeg	47.53 (44.76)	52.10 (50.84)
+ wav2bnd	40.45 (38.08)	44.18 (43.08)
+ wav2bnd-large	39.11 (36.43)	43.75 (42.59)
GradSeg	47.53 (44.76)	52.10 (50.84)
+ JSTTI E2E-refinement	44.47 (42.02)	50.87 (49.79)
Forced Alignment	<u>18.06 (18.41)</u>	<u>20.89 (21.30)</u>

By comparing the WERs in Table I and the word boundary metrics in Table II, we see that more accurate word boundaries usually lead to reduced WERs, especially as we gradually improve the word boundaries obtained from GradSeg with *wav2bnd*, *JSTTI E2E-refinement* and *wav2bnd-large* (c.f. Section III-E). Obtaining better word boundaries with XLS-R boundary self-training (*wav2bnd*) before our proposed JSTTI E2E-refinement routine is important, as jointly finetuning the CNN segmenter and the encoder model pre-trained using GradSeg boundaries (*GradSeg + JSTTI*

TABLE II
BOUNDARY TOKEN PRECISION (T-P) / RECALL (T-R) / F-1 (T-F1) IN PERCENTAGE (%) (WITH 20MS TOLERANCE) FOR UNSUPERVISED WORD BOUNDARIES OBTAINED. THE BEST RESULT IS SHOWN IN BOLD.

Method	T-P(↑)	T-R(↑)	T-F1(↑)
VG-HuBERT	24.94	21.18	22.91
GradSeg	36.21	36.51	36.36
+ wav2bnd	44.59	44.11	44.35
+ JSTTI E2E-refinement	63.17	63.56	63.36
+ wav2bnd-large	64.47	64.67	64.57
GradSeg	36.21	36.51	36.36
+ wav2bnd	44.59	44.11	44.35
+ wav2bnd-large	44.74	44.97	44.85
GradSeg	36.21	36.51	36.36
+ JSTTI E2E-refinement	37.94	39.03	38.48

E2E-refinement) is less effective than using *GradSeg + wav2bnd* boundaries (*GradSeg + wav2bnd + JSTTI E2E-refinement*). We also see that simply doing another run of boundary XLS-R self-training on top of the boundary predictions from *GradSeg + wav2bnd* (*GradSeg + wav2bnd + wav2bnd-large*) does not lead to a big improvement for the boundary metrics or the WERs.

We further demonstrate the effectiveness of pseudo-text self-training (c.f. Section III-F). We start from a pre-trained HuBERT-Large (300M) checkpoint and finetune the checkpoint under the CTC loss directly calculated on top of word token pseudo-targets. We repeat the same self-training routine on top of pseudo-transcripts obtained from two different word-level unsupervised ASR models, the JSTTI Transformer encoder and the PUSM model, and select from three different word boundary settings in Table I that are most insightful, namely, the forced alignment setting (top-line), the *GradSeg + wav2bnd + JSTTI E2E-refinement + wav2bnd-large* setting (best unsupervised word boundary setting; c.f. Table II) and the *GradSeg + wav2bnd + JSTTI E2E-refinement* setting (second-best unsupervised word boundary setting, with performance close to the best setting). We further provide an absolute top-line result where we finetune with the ground-truth paired transcript. Table III shows the results.

TABLE III

WERs FOR PUSM AND JSTTI-ENC MODELS USING DIFFERENT WORD BOUNDARY EXTRACTORS AFTER SELF-TRAINING. THE TWO TOP LINES HAVE BEEN UNDERLINED AND THE BEST RESULT FOR EACH MODEL IS SHOWN IN BOLD. THE TWO NUMBERS FOR THE ABSOLUTE TOP-LINE ARE THE SAME, AS NO PSEUDO-TRANSCRIPTS HAVE BEEN USED.

Method	WER-JSTTI-ENC(↓)	WER-PUSM(↓)
GradSeg		
+ wav2bnd	21.65	29.40
+ JSTTI E2E-refinement		
+ wav2bnd-large	20.68	28.87
Forced Alignment	<u>12.99</u>	<u>18.33</u>
Ground-Truth Transcripts	<u>1.08</u>	<u>1.08</u>

As expected, pseudo-text self-training further brings down the WERs of all selected settings and is more effective for the JSTTI-ENC model than for the PUSM model. With self-training, we obtain a final WER of 20.69% without resorting to using forced

TABLE IV
PSEUDO WERs FROM THE THREE DIFFERENT WORD BOUNDARY SETTINGS IN TABLE III. PSEUDO WERs ARE CALCULATED BY TREATING THE PSEUDO-TRANSCRIPTS AS REFERENCES AND THE PREDICTIONS FROM THE SELF-TRAINED HUBERT-LARGE MODELS AS HYPOTHESES.

Method	PWER-JSTTI-ENC(↓)	PWER-PUSM(↓)
GradSeg		
+ wav2bnd	19.76	14.14
+ JSTTI E2E-refinement		
+ wav2bnd-large	16.45	11.30
Forced Alignment	12.17	7.82

alignments. We additionally find that there are strong positive correlations between the pseudo WERs calculated between the word sequence predictions from the self-trained HuBERT-Large model and the pseudo-targets (reported in Table IV), the pseudo-target WERs calculated between the pseudo-targets and the ground-truth transcripts (main results reported in Table I), and the final WERs calculated between the word sequence predictions from the self-trained HuBERT-Large model and the ground-truth transcripts (reported in Table III), for both the JSTTI-ENC model and the PUSM model individually, but *not* across the two models. This observation shows that the pseudo WER logged during pseudo-text self-training could serve as an unsupervised metric. Unfortunately, obtaining this unsupervised metric is computationally intensive, and we leave a more detailed exploration of universal and efficient unsupervised metrics to future work.

Finally, comparing the WERs of our newly proposed JSTTI-ENC model and the (modified) PUSM model, we see that the unsupervised word-level ASR system trained under joint speech-text reconstruction yields significantly lower WERs, which we attribute to the intermediate encoder layer’s capability to capture a shared speech-text hidden space that emerges from just unimodal masked reconstruction tasks under a shared architecture. Pseudo-text self-training further increases the gap between JSTTI-ENC and PUSM and shows that the pseudo-transcripts provided by the JSTTI-ENC model exhibit transcription errors that are easier to correct under comparable settings. We additionally note that our attempts at designing a similar end-to-end differentiable boundary refinement routine based on PUSM did not work out due to instability issues. Instead, to train PUSM models, we directly extract discrete word-level speech token sequences (c.f. Section III-B) with the same boundaries used by JSTTI models for all comparisons. In future work, we plan to unify the two models to reduce the WERs further.

C. Ablation: Modifying PUSM Statistics Collection and Gradient Update Leads to Stronger Baselines

We show that our two-step update strategy in Section III-C that allows calculating the gradient over an arbitrarily large batch size creates a stronger baseline for the PUSM model. We compare three training settings:

- A fixed batch size of 6000, chosen so that the empirical position unigram and the empirical skipgram calculated for every speech sample in the batch, as well as all the associated gradient graphs, lie just below the total GPU memory of a 32GB V100 GPU (denoted as WER-6k);

- A fixed batch size of 6000, but only one single update is made after accumulating the gradient across 20 batches (denoted WER-6k-20); note that this setting is not as effective as using an effective batch size of 12,000, as accumulating the gradients of the L1 norms (Eqs. (4) and (5)) across multiple batches is not equivalent to accumulating the position-unigram and skipgram statistics across batches;
- The proposed modified training pipeline that allows the use of a true effective batch size of around 120000, as we separate position unigram + skipgram estimation and gradient update into two epochs (denoted WER-120k).

We repeat the three training settings under four unsupervised word boundaries for extracting speech tokens and show the comparison in Table V.

TABLE V
WERS FOR PUSM MODELS TRAINED UNDER THE MODIFIED UPDATE STRATEGY AGAINST TWO BASELINES. THE BEST RESULT FOR EACH WORD BOUNDARY SETTING IS SHOWN IN BOLD.

Method	WER-6k(↓)	WER-6k-20(↓)	WER-120k(↓)
GradSeg + wav2bnd	52.33	51.27	44.18
+ JSTTI E2E-refinement	41.29	40.62	34.08
+ wav2bnd-large	39.60	38.75	32.11
Forced Alignment	24.46	23.91	20.89

We see that the *WER-120k* strategy leads to a consistent 14-18% relative reduction in WERs, compared to using a fixed batch size of 6000, showing that having a large effective batch size is crucial to the PUSM method for word-level unsupervised ASR. On the other hand, *WER-6k-20* offers limited performance gain, showing that simple gradient accumulation is still limited by the large estimation errors of position-unigram and skipgram statistics on small batches.

D. Ablation: VG-HuBERT features vs HuBERT-Large features for Word-level Unsupervised ASR

We would like to understand if speech features from a visually grounded word discovery model trained with weakly labeled speech-image pairs offer any benefit for the word-level unsupervised ASR task. Table VI reports the WERs when we switch to frame-level features extracted from VG-HuBERT (from the 10th layer of a public VG-HuBERT₃ checkpoint [15]). Comparing the rows in Table VI with the relevant rows in Table I, we see that word-level features based on VG-HuBERT are less effective than those based on HuBERT-Large, regardless of what word boundaries we use to pool the word-level features. Despite the performance lag in all settings, applying *JSTTI E2E-refinement* with VG-HuBERT features, together with the subsequent iteration of *wav2bnd-large* training (c.f. Section III-E), still reduces the WER significantly. We additionally note that *JSTTI E2E-refinement* with VG-HuBERT frame-level features did not improve the word token F1: the F1 score dropped to 35.59% after *JSTTI E2E-refinement* and only rose to 42.86% after *wav2bnd-large*. This is expected as the VG-HuBERT model’s contextualization tends to push word identity information towards the temporal center of each word [15]. We conclude that *JSTTI E2E-refinement* and *wav2bnd* refinement can automatically extract *feature-specific* word-level information.

TABLE VI
WERS OBTAINED WITH JSTTI-ENC AND PUSM MODELS WITH DIFFERENT WORD BOUNDARIES, USING VG-HUBERT FEATURES (FLAGGED WITH “-VG”). THE TOP-LINE HAS BEEN UNDERLINED AND THE BEST RESULT FOR EACH MODEL IS SHOWN IN BOLD.

Method	WER-JSTTI-ENC-VG(↓)	WER-PUSM-VG(↓)
VG-HuBERT	50.39 (50.26)	56.44 (56.43)
GradSeg	50.90 (47.47)	53.54 (51.35)
+ wav2bnd	44.10 (41.31)	47.20 (45.79)
+ JSTTI E2E-refinement	36.29 (35.52)	38.43 (38.31)
+ wav2bnd-large	33.25 (31.55)	37.03 (36.55)
Forced Alignment	<u>22.06 (22.85)</u>	<u>25.26 (25.53)</u>

E. Ablation: Encoder-only vs Encoder-decoder Model for Word-level Unsupervised ASR

To understand if the specific architecture design affects word-level unsupervised ASR performance under the JSTTI task, we compare the JSTTI-ENC model to a one-layer encoder-decoder model with a similar number of parameters. For slightly better convergence, we modify the masking strategy in Section III-D for the encoder-decoder model: first, we replace every selected token span for masking with a single <MASK> token, and similarly for every selected token span for random replacement; second, we add insertion noise for the remainder of the masking budget. During training, the encoder-decoder optimizes the combined reconstruction loss using the original speech and text sequences as targets. We calculate the average teacher-forcing speech-to-text accuracy using paired validation data to record model checkpoints. During inference, to avoid decoder hallucination, we develop an encoder state matching method to construct a speech-to-text token dictionary inspired by unsupervised word translation [38]:

- 1) Feed every speech and text discrete token sequence into the encoder;
- 2) Extract speech token embedding by averaging the corresponding encoder state for each discrete speech token;
- 3) Extract text word token embedding by averaging the corresponding encoder state for each word token;
- 4) For each speech token embedding mean-pooled over the speech encoder states, query the top-1 text word token embedding mean-pooled over the text encoder states;
- 5) Use the constructed speech-text dictionary for word-level unsupervised ASR.

We report the comparison under different boundary settings in Table VII. Note that the basic JSTTI encoder-decoder model can be similarly augmented with *JSTTI E2E-refinement* and *wav2bnd-large* refinement (c.f. Section III-E), and the corresponding results are additionally reported in Table VII. Running *JSTTI E2E-refinement* and *wav2bnd-large* refinement with the encoder-decoder model gives us a total of two additional sets of word boundaries, and we further compare the quality of these new boundaries with those obtained with the encoder-only model in Table VIII.

Table VII shows that the JSTTI-ENC-DEC model combined with the encoder state matching method generally gives worse error rates. We believe this is because the encoder-only model directly applies the text output layer to the first encoder layer and could better utilize

TABLE VII

WERs OBTAINED WITH THE JSTTI-ENC AND THE JSTTI-ENC-DEC MODELS UNDER DIFFERENT WORD BOUNDARIES. WE UNDERLINE THE TOP-LINE RESULTS, AND THE LOWER WER WITHIN EACH ROW IS SHOWN IN BOLD.

Method	WER-ENC(↓)	WER-ENC-DEC(↓)
VG-HuBERT	47.99 (47.99)	56.14 (56.24)
GradSeg	47.53 (44.76)	55.46 (53.42)
+ wav2bnd	40.45 (38.08)	47.60 (46.03)
+ JSTTI E2E-refinement	30.97 (29.39)	39.97 (39.23)
+ wav2bnd-large	28.00 (26.51)	34.61 (33.97)
Forced Alignment	18.06 (18.41)	27.16 (26.98)

TABLE VIII

WERs OBTAINED WITH THE JSTTI-ENC AND THE JSTTI-ENC-DEC MODELS AFTER THEY ARE RE-TRAINED ON TOP OF THE TWO SETS OF REFINED WORD BOUNDARIES OBTAINED WITH JSTTI-ENC AND THE TWO ADDITIONAL SETS OF REFINED BOUNDARIES OBTAINED WITH JSTTI-ENC-DEC

Method	WER-ENC(↓)	WER-ENC-DEC(↓)
GradSeg		
+ wav2bnd		
+ JSTTI E2E-refinement (w/ JSTTI-ENC-DEC)*	30.50 (28.96)	37.64 (36.82)
+ wav2bnd-large	27.97 (26.47)	34.61 (33.97)
GradSeg		
+ wav2bnd		
+ JSTTI E2E-refinement (w/ JSTTI-ENC)*	29.90 (28.26)	37.16 (36.17)
+ wav2bnd-large	28.00 (26.51)	35.08 (34.15)

contextualized representation during evaluation, while the encoder state matching method used for evaluating the encoder-decoder model cannot.

By comparing the WERs in the first row and third row of Table VIII within either the left or right column, we see that both the encoder-decoder architecture and the encoder-only architecture are almost equally capable of refining the initial *GradSeg + wav2bnd* word boundaries via the JSTTI E2E-refinement routine. This continues to hold as we further apply *wav2bnd-large* refinement, as shown in the second row and the fourth row of Table VIII within either the left or right column.

F. Ablation: Regularization Sensitivity for JSTTI E2E-Refinement

We add the word count loss and the word frequency loss (c.f. Eqs. (17), (18) and (19)) for our JSTTI E2E-refinement routine (c.f. Section III-E) to improve the word-level segmental structure. To show that adding this regularization is crucial, we repeat the refinement routine with three distinct sets of regularization strengths. We denote them as *small regularization* with $\gamma_1 = 5, \gamma_2 = 5000$, *medium regularization* with $\gamma_1 = 50, \gamma_2 = 500000$ and *strong regularization* with $\gamma_1 = 50000, \gamma_2 = 50000000$. The *medium regularization* setting here corresponds to what is reported for the setting *GradSeg + wav2bnd + JSTTI E2E-refinement* in Tables I and II. The three runs are reported in Table IX.

From Table IX, we see that performance is harmed by setting the regularization coefficients γ_1 and γ_2 too small, but that setting them too large is not greatly detrimental.

TABLE IX

WERs FOR THE JSTTI-ENC MODEL FOR THE GRADSEG + WAV2BND + JSTTI E2E-REFINEMENT METHOD UNDER THREE DIFFERENT REGULARIZATION STRENGTHS. THE BEST RESULTS ARE SHOWN IN BOLD

Regularization Strength	WER-JSTTI-ENC(↓)	Token F-1(↑)
Small Regularization	35.25 (33.25)	58.27
Medium Regularization	30.97 (29.39)	63.36
Strong Regularization	30.97 (29.18)	63.31

G. Ablation: Choice of Word-level Clusters for Speech Quantization

Throughout our experiments, we used different sets of word boundaries for temporal pooling of the word-level feature vectors but kept the cluster centroids fixed across the speech token extraction process (c.f. Section III-B). These cluster centroids were obtained by training a k-means model on top of word-level speech feature vectors mean-pooled using the word boundaries predicted by VG-HuBERT. We denote cluster centroids obtained this way as VG-HuBERT-induced cluster centroids. Doing so saved training time as we could simply finetune a previous JSTTI-ENC model checkpoint once better-quality speech token sequences become available. To show that this choice is indeed optimal, we train the JSTTI-ENC model and the PUSM model in six different settings as shown below, and the results are reported in Table X:

- 1) Forced aligned boundaries for extracting word-level features & forced alignment induced cluster centroids (FA BND & Matched CLUS)
- 2) Forced aligned boundaries for extracting continuous word-level features & VG-HuBERT induced cluster centroids (FA BND & VG-HUBERT CLUS)
- 3) *GradSeg + wav2bnd* boundaries for extracting continuous word-level features & *GradSeg + wav2bnd* induced cluster centroids (*GradSeg + wav2bnd* BND & Matched CLUS)
- 4) *GradSeg + wav2bnd* boundaries for extracting continuous word-level features & VG-HuBERT induced cluster centroids (*GradSeg + wav2bnd* BND & VG-HuBERT CLUS)
- 5) *GradSeg + wav2bnd + JSTTI E2E-refinement + wav2bnd-large* boundaries for extracting continuous word-level features & *GradSeg + wav2bnd + JSTTI E2E-refinement + wav2bnd-large* induced cluster centroids (*GradSeg + wav2bnd + JSTTI E2E-refinement + wav2bnd-large* BND & Matched CLUS)
- 6) *GradSeg + wav2bnd + JSTTI E2E-refinement + wav2bnd-large* boundaries for extracting continuous word-level features & VG-HuBERT induced cluster centroids (*GradSeg + wav2bnd + JSTTI E2E-refinement + wav2bnd-large* BND & VG-HUBERT CLUS)

For settings 3 and 4, we further compare the differences when we further train the JSTTI-ENC model under the JSTTI E2E-refinement routine (c.f. Section III-E) when we use different cluster centroids for speech word-level token quantization.

Table X shows that we rarely get any benefit if we were to switch away from using VG-HuBERT-induced cluster centroids for almost all word boundary settings, except when we have word boundaries from forced alignments (and even then, the improvement is minimal). We even saw a noticeable increase in WER for setting 3 (in rows 3 and 5) when matched cluster centroids were used instead of VG-HuBERT-induced centroids for the JSTTI-ENC model.

TABLE X

WERS OBTAINED WITH THE JSTTI-ENC AND THE PUSM MODELS, TRAINED USING DISCRETE SPEECH CLUSTER SEQUENCES OBTAINED WITH DIFFERENT PAIRS OF BOUNDARIES AND CLUSTER CENTROIDS. THE RESULT WITH A LOWER WER FOR EACH PAIRWISE COMPARISON IS SHOWN IN BOLD.

Settings	WER-JSTTI-ENC(↓)	WER-PUSM(↓)
FA BND & Matched CLUS	17.86 (18.23)	20.20 (20.60)
FA BND & VG-HUBERT CLUS	18.06 (18.41)	20.89 (21.30)
<i>GradSeg</i> + <i>wav2bnd</i> BND & Matched CLUS	45.21 (43.50)	45.91 (45.46)
<i>GradSeg</i> + <i>wav2bnd</i> BND & VG-HUBERT CLUS	40.45 (38.08)	44.18 (43.08)
<i>GradSeg</i> + <i>wav2bnd</i> BND & Matched CLUS (w/ JSTTI E2E-refinement)	38.89 (37.31)	39.71 (39.32)
<i>GradSeg</i> + <i>wav2bnd</i> BND & VG-HUBERT CLUS (w/ JSTTI E2E-refinement)	30.97 (29.39)	34.08 (33.71)
<i>GradSeg</i> + <i>wav2bnd</i> + <i>JSTTI E2E-refinement</i> + <i>wav2bnd-large</i> BND & Matched CLUS	28.97 (27.63)	32.44 (32.35)
<i>GradSeg</i> + <i>wav2bnd</i> + <i>JSTTI E2E-refinement</i> + <i>wav2bnd-large</i> BND & VG-HuBERT CLUS	28.00 (26.51)	32.11 (31.91)

H. Analysis: Effect of Boundary Error on Distribution Matching Model Parameter Optimization

Previously, in Section IV-B, we see that the *JSTTI E2E-refinement* boundary refinement process depends on the quality of the initial word boundaries: the E2E refinement algorithm can achieve better results when initialized using *GradSeg* + *wav2bnd* than when initialized using *GradSeg*. We wish to determine whether this sensitivity to initial conditions also characterizes the relationship between training and evaluation data, i.e., if the evaluation data are more accurately segmented than the training data, can the model take advantage of the improvement? Table XI shows WERs achieved by models trained using discrete speech sequences obtained from worse boundaries (four different boundary settings listed in the Table) but evaluated using speech token sequences obtained from better boundaries (from *GradSeg* + *wav2bnd* + *JSTTI E2E-refinement* + *wav2bnd-large*).

TABLE XI

WERS FOR THE JSTTI-ENC AND PUSM MODELS AS WE FEED MODELS TRAINED WITH WORSE-QUALITY SPEECH TOKEN SEQUENCES (AS SHOWN) BUT TESTED WITH MORE ACCURATELY SEGMENTED SPEECH TOKENS (*GradSeg* + *wav2bnd* + *JSTTI E2E-refinement* + *wav2bnd-large* IN ALL CASES).

Method	WER-JSTTI-ENC(↓)	WER-PUSM(↓)
<i>GradSeg</i>	29.59 (28.29)	35.18 (34.89)
+ <i>wav2bnd</i>	29.40 (28.00)	33.82 (33.58)
+ <i>JSTTI E2E-refinement</i> *	28.09 (26.85)	32.39 (32.15)
+ <i>wav2bnd-large</i>	28.00 (26.51)	32.11 (31.91)

We see that for both models and training algorithms, just by replacing word-level speech tokens used for evaluation with those obtained with more accurate word boundaries, the WERs of best and worst settings are within 6-7% of each other for the JSTTI-ENC

model and within 9-10% for the PUSM model. We conclude that the learning process of the Transformer encoder parameters for both the JSTTI-ENC and PUSM models is not too sensitive to bad word boundaries during training. Hence, both models could be used to directly evaluate better-quality word-level speech token sequences as they become available.

I. Analysis: JSTTI-ENC Model Layer-wise Performance

We try to understand why the model's first encoder layer offers better contextualized speech representations during the speech-to-text evaluation stage of the JSTTI-ENC model, despite the fact that the representation from the second layer is used during the training stage (under joint speech-to-speech token infilling and text-to-text token infilling). We show the evaluation set WERs and training set WERs when speech representations from either the first or the second encoder layer are fed into the text output layer for the word-level unsupervised ASR task, under different word boundary settings. We report the results under five different boundary settings in Tables XII and XIII.

TABLE XII

WERS FOR THE JSTTI-ENC MODEL WHEN WE FEED EITHER LAYER ONE OR LAYER TWO SPEECH FEATURES FROM THE EVALUATION SET TO THE TEXT OUTPUT LAYER (WER-L1-EVAL AND WER-L2-EVAL, RESPECTIVELY). THE BETTER RESULTS WITHIN EACH ROW ARE SHOWN IN BOLD.

Method	WER-L1-EVAL(↓)	WER-L2-EVAL(↓)
<i>GradSeg</i>	47.53 (44.76)	56.66 (54.59)
+ <i>wav2bnd</i>	40.45 (38.08)	49.79 (48.02)
+ <i>JSTTI E2E-refinement</i> *	29.90 (28.26)	40.43 (39.02)
+ <i>wav2bnd-large</i>	28.00 (26.51)	38.74 (37.57)
Forced Alignment	18.06 (18.41)	27.76 (28.00)

TABLE XIII

WERS FOR THE JSTTI-ENC MODEL WHEN WE FEED EITHER LAYER ONE OR LAYER TWO SPEECH FEATURES FROM THE TRAINING SET TO THE TEXT OUTPUT LAYER (WER-L1-TRAIN AND WER-L2-TRAIN, RESPECTIVELY). THE BETTER RESULTS WITHIN EACH ROW ARE SHOWN IN BOLD.

Method	WER-L1-TRAIN(↓)	WER-L2-TRAIN(↓)
<i>GradSeg</i>	46.44 (43.55)	50.97 (48.41)
+ <i>wav2bnd</i>	39.09 (36.69)	43.66 (41.54)
+ <i>JSTTI E2E-refinement</i> *	28.31 (26.61)	32.73 (30.89)
+ <i>wav2bnd-large</i>	26.57 (24.92)	30.85 (29.11)
Forced Alignment	16.58 (16.92)	19.89 (20.18)

From Tables XII and XIII, we see that feeding the contextualized speech representations from the first encoder layer into the text output layer consistently shows significantly better performance on both the training set and the evaluation set. Comparing the respective entries among the two tables, we see that using the second encoder layer's representations exhibits significantly worse over-fitting on the training set, while the amount of over-fitting is more subdued if the representations from the first layer are used. We hypothesize that after JSTTI training, the first encoder layer learns a more universal representation that is shared between the speech and text modalities, while the representations from the second layer tend to be modality-specific.

To further showcase that the first encoder layer indeed learns a shared speech-text representation, we report the cross-modal word purity (WP), cross-modal cluster purity (CP), and the cross-modal word-normalized mutual information (WNMI), similarly defined as in [2] to measure the quality of the discrete representation of layer-wise features. To calculate these metrics, we first extract contextualized word-level speech features and text features on the entire training set of discrete word-level speech token sequences and word-level text, from either layer one or layer two of the JSTTI-ENC model. We then perform k-means clustering on the extracted contextualized *speech* representations (with $k = 1024$) and obtain a set of cluster centroids. Finally, we quantize the extracted *text* representations with this set of cluster centroids. Denote Y_t as a word label in text and L_t as the corresponding k-means label obtained from the above routine. We define the empirical joint probability \hat{P}_{YL} , as

$$\hat{P}_{YL}(i,j) = \frac{\sum_{t=1}^T [Y_t = i \wedge L_t = j]}{T} \quad (20)$$

where T is the total number of extracted word-level representations in the training set. From the joint probability, we can compute the mostly likely word label $Y^*(j)$ for each k-means label j , and the most likely k-means label $L^*(i)$ for each word label i as:

$$L^*(i) = \operatorname{argmax}_j \hat{P}_{YL}(i,j) \quad (21)$$

$$Y^*(j) = \operatorname{argmax}_i \hat{P}_{YL}(i,j). \quad (22)$$

We can define word purity (WP), cluster purity (CP), and word-normalized mutual information (WNMI) as:

$$\text{WP} = \mathbb{E}_{\hat{P}_L(j)} [\hat{P}_{Y|L}(Y^*(j)|j)] \quad (23)$$

$$\text{CP} = \mathbb{E}_{\hat{P}_Y(i)} [\hat{P}_{L|Y}(L^*(i)|i)] \quad (24)$$

$$\text{WNMI} = \frac{I(Y;L)}{H(Y)} = - \frac{\sum_i \sum_j \hat{P}_{YL}(i,j) \log \frac{\hat{P}_{YL}(i,j)}{\hat{P}_Y(i) \hat{P}_L(j)}}{\sum_i \hat{P}_Y(i) \log \hat{P}_Y(i)} \quad (25)$$

where we denote the marginal distribution over k-means label j as $\hat{P}_L(j)$, the marginal distribution over word label i as $\hat{P}_Y(i)$, the conditional probability of a word label i given a k-means label j as $\hat{P}_{Y|L}(i|j)$, the conditional probability of a k-means label j given a word label i as $\hat{P}_{L|Y}(j|i)$, the mutual information between Y and L as $I(Y;L)$ and the entropy of Y as $H(Y)$. WP can be interpreted as the word accuracy if we transcribe each k-means class with its most likely word label. CP is the counterpart of WP and measures the average probability that the same word is labeled as the same k-means class. WNMI is an information-theoretic metric that measures the percentage of uncertainty eliminated for a word label Y after observing its k-means label L [2]. We only report these metrics in Table XIV for the setting trained with word-level speech token sequences obtained under the boundary setting denoted as *GradSeg + wav2bnd + JSTTI E2E-refinement + wav2bnd-large* (c.f. Section III-E), as results obtained under other settings are similar. Table XIV shows better cross-modal WP, CP, and WNMI for layer one rather than layer two, again solidifying the hypothesis that layer one learns a shared representation between speech and text modalities, while the representations from layer 2 are less shared across the two modalities.

TABLE XIV

WP, CP, AND WNMI CALCULATED WITH CROSS-MODAL QUANTIZATION ON TOP OF LAYER ONE (L1) AND LAYER ONE (L2) FEATURES EXTRACTED WITH JSTTI-ENC MODEL ON THE TRAINING SET. THE BETTER RESULTS AMONG THE TWO LAYERS ARE SHOWN IN BOLD.

Layer	WP(↑)	CP(↑)	CWMI(↑)
L1	0.831	0.550	0.855
L2	0.581	0.378	0.577

V. CONCLUSION

This work is the first step toward solving the word-level unsupervised ASR task. We curated a simplified corpus for this new task and proposed solving the unsupervised ASR problem with the joint speech-text token-infilling (JSTTI) Transformer. Our new model consistently beat our enhanced baseline model called position-unigram and skipgram matching (PUSM), and the performance could be further improved as we iteratively refine the word-level segmental structure. Through extensive experiments, we demonstrated the validity of our model pipeline and design choices. In future work, we plan to extend our vocabulary size by working with sub-word units, develop efficient universal unsupervised model selection metrics, and test our methods in truly unpaired settings.

ACKNOWLEDGMENTS

This research was supported in part by a grant from the Institute for Information & Communication Technology Promotion (IITP). All findings and opinions are those of the authors and are not endorsed by IITP.

REFERENCES

- [1] A. Baevski, Y. Zhou, A. Mohamed, and M. Auli, “wav2vec 2.0: A framework for self-supervised learning of speech representations,” in *Advances in Neural Information Processing Systems 33: Annual Conference on Neural Information Processing Systems 2020, NeurIPS 2020, December 6-12, 2020, virtual*, H. Larochelle, M. Ranzato, R. Hadsell, M. Balcan, and H. Lin, Eds., 2020, pp. 12 449–12 460.
- [2] W. Hsu, B. Bolte, Y. H. Tsai, K. Lakhotia, R. Salakhutdinov, and A. Mohamed, “HuBERT: Self-supervised speech representation learning by masked prediction of hidden units,” *IEEE ACM Trans. Audio Speech Lang. Process.*, vol. 29, pp. 3451–3460, 2021.
- [3] A. Babu, C. Wang, A. Tjandra, K. Lakhotia, Q. Xu, N. Goyal, K. Singh, P. von Platen, Y. Saraf, J. Pino, A. Baevski, A. Conneau, and M. Auli, “XLS-R: self-supervised cross-lingual speech representation learning at scale,” in *Interspeech 2022, 23rd Annual Conference of the International Speech Communication Association, Incheon, Korea, 18-22 September 2022*, H. Ko and J. H. L. Hansen, Eds. ISCA, 2022, pp. 2278–2282.
- [4] D. Liu, K. Chen, H. Lee, and L. Lee, “Completely unsupervised phoneme recognition by adversarially learning mapping relationships from audio embeddings,” in *Interspeech 2018, 19th Annual Conference of the International Speech Communication Association, Hyderabad, India, 2-6 September 2018*, B. Yegnanarayana, Ed. ISCA, 2018, pp. 3748–3752.
- [5] C. Yeh, J. Chen, C. Yu, and D. Yu, “Unsupervised speech recognition via segmental empirical output distribution matching,” in *7th International Conference on Learning Representations, ICLR 2019, New Orleans, LA, USA, May 6-9, 2019*. OpenReview.net, 2019. [Online]. Available: <https://openreview.net/forum?id=Bylmkh05KX>
- [6] K. Chen, C. Tsai, D. Liu, H. Lee, and L. Lee, “Completely unsupervised phoneme recognition by a generative adversarial network harmonized with iteratively refined hidden markov models,” in *Interspeech 2019, 20th Annual Conference of the International Speech Communication Association, Graz, Austria, 15-19 September 2019*, G. Kubin and Z. Kacic, Eds. ISCA, 2019, pp. 1856–1860.

- [7] A. Baevski, W. Hsu, A. Conneau, and M. Auli, "Unsupervised speech recognition," in *Advances in Neural Information Processing Systems 34: Annual Conference on Neural Information Processing Systems 2021, NeurIPS 2021, December 6-14, 2021, virtual*, M. Ranzato, A. Beygelzimer, Y. N. Dauphin, P. Liang, and J. W. Vaughan, Eds., 2021, pp. 27 826–27 839.
- [8] A. H. Liu, W. Hsu, M. Auli, and A. Baevski, "Towards end-to-end unsupervised speech recognition," in *IEEE Spoken Language Technology Workshop, SLT 2022, Doha, Qatar, January 9-12, 2023*. IEEE, 2022, pp. 221–228.
- [9] L. Wang, J. Ni, H. Gao, J. Li, K. C. Chang, X. Fan, J. Wu, M. Hasegawa-Johnson, and C. Yoo, "Listen, decipher and sign: Toward unsupervised speech-to-sign language recognition," in *Findings of the Association for Computational Linguistics: ACL 2023*. Toronto, Canada: Association for Computational Linguistics, Jul. 2023, pp. 6785–6800.
- [10] L. Wang, M. Hasegawa-Johnson, and C. D. Yoo, "Unsupervised speech recognition with n-skipgram and positional unigram matching," in *ICASSP 2024-2024 IEEE International Conference on Acoustics, Speech and Signal Processing (ICASSP)*. IEEE, 2024, pp. 10 936–10 940.
- [11] M. Hasegawa-Johnson, L. Rolston, C. Goudeseune, G.-A. Levow, and K. Kirchhoff, "Grapheme-to-phoneme transduction for cross-language asr," in *Statistical Language and Speech Processing*, L. Espinosa-Anke, C. Martín-Vide, and I. Spasić, Eds. Springer International Publishing, 2020, pp. 3–19.
- [12] J. Ni, L. Wang, H. Gao, K. Qian, Y. Zhang, S. Chang, and M. Hasegawa-Johnson, "Unsupervised text-to-speech synthesis by unsupervised automatic speech recognition," in *Interspeech 2022, 23rd Annual Conference of the International Speech Communication Association, Incheon, Korea, 18-22 September 2022*, H. Ko and J. H. L. Hansen, Eds. ISCA, 2022, pp. 461–465.
- [13] A. Pasad, B. Shi, and K. Livescu, "Comparative layer-wise analysis of self-supervised speech models," *CoRR*, vol. abs/2211.03929, 2022. [Online]. Available: <https://doi.org/10.48550/arXiv.2211.03929>
- [14] D. Gao, J. Shi, S. Chuang, L. P. García, H. Lee, S. Watanabe, and S. Khudanpur, "Euro: ESPnet unsupervised ASR open-source toolkit," in *IEEE International Conference on Acoustics, Speech and Signal Processing ICASSP 2023, Rhodes Island, Greece, June 4-10, 2023*. IEEE, 2023, pp. 1–5.
- [15] P. Peng and D. Harwath, "Word discovery in visually grounded, self-supervised speech models," in *Interspeech 2022, 23rd Annual Conference of the International Speech Communication Association, Incheon, Korea, 18-22 September 2022*, H. Ko and J. H. L. Hansen, Eds. ISCA, 2022, pp. 2823–2827.
- [16] S. Bhati, J. Villalba, P. Zelasko, L. Moro-Velázquez, and N. Dehak, "Unsupervised speech segmentation and variable rate representation learning using segmental contrastive predictive coding," *IEEE ACM Trans. Audio Speech Lang. Process.*, vol. 30, pp. 2002–2014, 2022.
- [17] L. Tseng, E. Hu, D. C. Chiang, Y. Tseng, H. Lee, L. Lee, and S. Sun, "REBORN: reinforcement-learned boundary segmentation with iterative training for unsupervised ASR," *CoRR*, vol. abs/2402.03988, 2024. [Online]. Available: <https://doi.org/10.48550/arXiv.2402.03988>
- [18] R. Algayres, P. Diego-Simon, B. Sagot, and E. Dupoux, "XLS-R fine-tuning on noisy word boundaries for unsupervised speech segmentation into words," in *Findings of the Association for Computational Linguistics: EMNLP 2023, Singapore, December 6-10, 2023*, H. Bouamor, J. Pino, and K. Bali, Eds. Association for Computational Linguistics, 2023, pp. 12 103–12 112.
- [19] A. Conneau, A. Baevski, R. Collobert, A. Mohamed, and M. Auli, "Unsupervised cross-lingual representation learning for speech recognition," *CoRR*, vol. abs/2006.13979, 2020. [Online]. Available: <https://arxiv.org/abs/2006.13979>
- [20] S. Chen, C. Wang, Z. Chen, Y. Wu, S. Liu, Z. Chen, J. Li, N. Kanda, T. Yoshioka, X. Xiao, J. Wu, L. Zhou, S. Ren, Y. Qian, Y. Qian, J. Wu, M. Zeng, X. Yu, and F. Wei, "WavLM: Large-scale self-supervised pre-training for full stack speech processing," *IEEE J. Sel. Top. Signal Process.*, vol. 16, no. 6, pp. 1505–1518, 2022.
- [21] J. Ao, R. Wang, L. Zhou, C. Wang, S. Ren, Y. Wu, S. Liu, T. Ko, Q. Li, Y. Zhang, Z. Wei, Y. Qian, J. Li, and F. Wei, "SpeechT5: Unified-modal encoder-decoder pre-training for spoken language processing," in *Proceedings of the 60th Annual Meeting of the Association for Computational Linguistics (Volume 1: Long Papers), ACL 2022, Dublin, Ireland, May 22-27, 2022*, S. Muresan, P. Nakov, and A. Villavicencio, Eds. Association for Computational Linguistics, 2022, pp. 5723–5738.
- [22] Z. Zhang, L. Zhou, J. Ao, S. Liu, L. Dai, J. Li, and F. Wei, "SpeechUT: Bridging speech and text with hidden-unit for encoder-decoder based speech-text pre-training," in *Proceedings of the 2022 Conference on Empirical Methods in Natural Language Processing, EMNLP 2022, Abu Dhabi, United Arab Emirates, December 7-11, 2022*, Y. Goldberg, Z. Kozareva, and Y. Zhang, Eds. Association for Computational Linguistics, 2022, pp. 1663–1676.
- [23] Z. Zhang, S. Chen, L. Zhou, Y. Wu, S. Ren, S. Liu, Z. Yao, X. Gong, L. Dai, J. Li, and F. Wei, "SpeechLM: Enhanced speech pre-training with unpaired textual data," *IEEE/ACM Transactions on Audio, Speech, and Language Processing*, vol. 32, pp. 2177–2187, 2024.
- [24] A. Bapna, Y. Chung, N. Wu, A. Gulati, Y. Jia, J. H. Clark, M. Johnson, J. Riesa, A. Conneau, and Y. Zhang, "SLAM: A unified encoder for speech and language modeling via speech-text joint pre-training," *CoRR*, vol. abs/2110.10329, 2021. [Online]. Available: <https://arxiv.org/abs/2110.10329>
- [25] Z. Chen, Y. Zhang, A. Rosenberg, B. Ramabhadran, P. J. Moreno, A. Bapna, and H. Zen, "MAESTRO: matched speech text representations through modality matching," in *Interspeech 2022, 23rd Annual Conference of the International Speech Communication Association, Incheon, Korea, 18-22 September 2022*, H. Ko and J. H. L. Hansen, Eds. ISCA, 2022, pp. 4093–4097.
- [26] M. Artetxe, G. Labaka, E. Agirre, and K. Cho, "Unsupervised neural machine translation," in *6th International Conference on Learning Representations, ICLR 2018, Vancouver, BC, Canada, April 30 - May 3, 2018, Conference Track Proceedings*. OpenReview.net, 2018. [Online]. Available: <https://openreview.net/forum?id=Sy2ogebAW>
- [27] G. Lample, A. Conneau, L. Denoyer, and M. Ranzato, "Unsupervised machine translation using monolingual corpora only," in *6th International Conference on Learning Representations, ICLR 2018, Vancouver, BC, Canada, April 30 - May 3, 2018, Conference Track Proceedings*. OpenReview.net, 2018. [Online]. Available: <https://openreview.net/forum?id=rkYTTf-AZ>
- [28] S. Cuervo, M. Grabias, J. Chorowski, G. Ciesielski, A. Lancucki, P. Rychlikowski, and R. Marxer, "Contrastive prediction strategies for unsupervised segmentation and categorization of phonemes and words," in *IEEE International Conference on Acoustics, Speech and Signal Processing, ICASSP 2022, Virtual and Singapore, 23-27 May 2022*. IEEE, 2022, pp. 3189–3193.
- [29] S. Cuervo, A. Lancucki, R. Marxer, P. Rychlikowski, and J. Chorowski, "Variable-rate hierarchical CPC leads to acoustic unit discovery in speech," in *NeurIPS*, 2022.
- [30] H. Kamper, "Word segmentation on discovered phone units with dynamic programming and self-supervised scoring," *IEEE ACM Trans. Audio Speech Lang. Process.*, vol. 31, pp. 684–694, 2023.
- [31] R. Algayres, T. Ricoul, J. Karadayi, H. Laurençon, S. Zaiem, A. Mohamed, B. Sagot, and E. Dupoux, "DP-parse: Finding word boundaries from raw speech with an instance lexicon," *Transactions of the Association for Computational Linguistics*, vol. 10, pp. 1051–1065, 2022. [Online]. Available: <https://aclanthology.org/2022.tacl-1.61>
- [32] T. S. Fuchs and Y. Hoshen, "Unsupervised word segmentation using temporal gradient pseudo-labels," in *IEEE International Conference on Acoustics, Speech and Signal Processing ICASSP 2023, Rhodes Island, Greece, June 4-10, 2023*. IEEE, 2023, pp. 1–5.
- [33] V. Panayotov, G. Chen, D. Povey, and S. Khudanpur, "Librispeech: An ASR corpus based on public domain audio books," in *ICASSP*, 2015, pp. 5206–5210.
- [34] M. Lewis, Y. Liu, N. Goyal, M. Ghazvininejad, A. Mohamed, O. Levy, V. Stoyanov, and L. Zettlemoyer, "BART: Denoising sequence-to-sequence pre-training for natural language generation, translation, and comprehension," in *Proceedings of the 58th Annual Meeting of the Association for Computational Linguistics*. Online: Association for Computational Linguistics, Jul. 2020, pp. 7871–7880.
- [35] Y. Bengio, "Deep learning of representations for unsupervised and transfer learning," in *Unsupervised and Transfer Learning - Workshop held at ICML 2011, Bellevue, Washington, USA, July 2, 2011*, ser. JMLR Proceedings, I. Guyon, G. Dror, V. Lemaire, G. W. Taylor, and D. L. Silver, Eds., vol. 27. JMLR.org, 2012, pp. 17–36.
- [36] A. Polyak, Y. Adi, J. Copet, E. Kharitonov, K. Lakhota, W. Hsu, A. Mohamed, and E. Dupoux, "Speech resynthesis from discrete disentangled self-supervised representations," in *Interspeech 2021, 22nd Annual Conference of the International Speech Communication Association, Brno, Czechia, 30 August - 3 September 2021*, H. Hermansky, H. Cernocký, L. Burget, L. Lamel, O. Scharenborg, and P. Motlíček, Eds. ISCA, 2021, pp. 3615–3619.
- [37] E. Dunbar, X. Cao, J. Benjumea, J. Karadayi, M. Bernard, L. Besacier, X. Anguera, and E. Dupoux, "The zero resource speech challenge 2017," *CoRR*, vol. abs/1712.04313, 2017. [Online]. Available: <http://arxiv.org/abs/1712.04313>
- [38] G. Lample, A. Conneau, M. Ranzato, L. Denoyer, and H. Jégou, "Word translation without parallel data," in *6th International Conference on Learning Representations, ICLR 2018, Vancouver, BC, Canada, April 30 - May 3, 2018, Conference Track Proceedings*. OpenReview.net, 2018. [Online]. Available: <https://openreview.net/forum?id=H196sainb>